

# Wet Polymeric Precipitation Synthesis for Monophasic Tricalcium Phosphate

I. Grigoravičiute-Puroniene, K. Tsuru, E. Garskaite, Z. Stankeviciute, A. Beganskiene, K. Ishikawa, A. Kareiva

**Abstract**—Tricalcium phosphate ( $\beta$ - $\text{Ca}_3(\text{PO}_4)_2$ ,  $\beta$ -TCP) powders were synthesized using wet polymeric precipitation method for the first time to our best knowledge. The results of X-ray diffraction analysis showed the formation of almost single  $\alpha$ -Ca-deficient hydroxyapatite (CDHA) phase of a poor crystallinity already at room temperature. With continuously increasing the calcination temperature up to 800 °C, the crystalline  $\beta$ -TCP was obtained as the main phase. It was demonstrated that infrared spectroscopy is very effective method to characterize the formation of  $\beta$ -TCP. The SEM results showed that  $\beta$ -TCP solids were homogeneous having a small particle size distribution. The  $\beta$ -TCP powders consisted of spherical particles varying in size from 100 to 300 nm. Fabricated  $\beta$ -TCP specimens were placed to the bones of the rats and maintained for 1-2 months.

**Keywords**— $\beta$ -TCP, bone regeneration, wet chemical processing, polymeric precipitation.

## I. INTRODUCTION

CALCIUM phosphate (CaP)-based ceramics are extensively employed in orthopedics and dental applications. Having a chemical composition very close to the mineral part of the bone, calcium hydroxyapatite (CHA,  $\text{Ca}_{10}(\text{PO}_4)_6(\text{OH})_2$ , with a Ca/P molar ratio equal to 1.67), tricalcium phosphates (TCP,  $\text{Ca}_3(\text{PO}_4)_2$ ) such as  $\alpha$ - or  $\beta$ -tricalcium phosphate ( $\alpha$ - or  $\beta$ -TCP), with a Ca/P molar ratio equal to 1.5)) and the so-called biphasic calcium phosphates (BCP, which is a blend of either  $\beta$ -TCP and CHA or  $\alpha$ -TCP and CHA) show excellent biocompatibility [1]-[3]. These CaPs have been applied clinically as bone substitutes, implants as well as coating of dental implants and metallic prosthesis [4]-[9]. Among above mentioned bioceramics, CHA is thermodynamically the most stable phase in physiological conditions and has the ability for direct chemical bonding to the bone, while  $\beta$ -TCP has attracted great attention because of its excellent *in vivo* bioresorbability leading to new bone growth replacing the implanted  $\beta$ -TCP [10]-[12]. In most cases, the  $\beta$ -TCP is implanted into a bone structure in the form of granules or blocks (dense or macroporous scaffolds) [13]-[15].

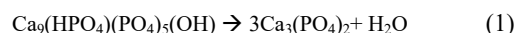
I. Grigoravičiute-Puroniene, A. Beganskiene, A. Kareiva are with Department of Inorganic Chemistry, Vilnius University, Naugarduko 24, Vilnius LT-03225, Lithuania (corresponding author; e-mail: aldona.beganskiene@chf.vu.lt)

K. Tsuru and K. Ishikawa are with Department of Biomaterials, Faculty of Dental Science, Kyushu University 3-1-1, Maidashi, Higashi-ku, Fukuoka 812-8582 Japan.

E. Garskaite and Z. Stankeviciute are with Department of Applied Chemistry, Vilnius University, Naugarduko 24, Vilnius LT-03225, Lithuania.

This work was supported by a grant KALFOS (No. LJB-2/2015) from the Research Council of Lithuania.

In the past decades,  $\beta$ -TCP powders are reportedly prepared via conventional solid-state reactions, combustion or flame spray synthesis, chemical precipitation technique, and sol-gel method [16]-[19]. Namely, the precipitation technique, besides its low cost, has been widely used due to the better control of composition and physical properties of obtained powders [19], [20]. This method has the attraction in that the chemical reagents are mixed intimately on a molecular level at an early stage of the process leading to the reactive precursor powders required for the synthesis of  $\beta$ -TCP at elevated temperatures [19]. Since  $\beta$ -TCP cannot be synthesized directly in aqueous solution, the compound that may precipitate is a CDHA ( $\text{Ca}_9(\text{HPO}_4)(\text{PO}_4)_5(\text{OH})$ ), which has the same crystal structure as CHA and the same Ca/P molar ratio as TCP. The crystallization of  $\beta$ -TCP requires further calcination of the apatite compound at temperatures over 700-800 °C. At such temperatures, the CDHA transforms into  $\beta$ -TCP with the loss of water [21], [22].



This two-step wet chemical precipitation method yields a material of high phase purity comprising the desired  $\beta$ -TCP phase. However, the phase purity of end product and repeatability of the synthesis procedure are very much dependent on different synthesis parameters. Therefore, the aim of this study was to develop a fast and effective precipitation technique for the fabrication of monophasic  $\beta$ -TCP powders. Since the parameters of sample preparation strongly affect the physicochemical properties of synthesized materials, the detailed procedure of our sample preparation is provided here. In addition, structural features, morphological characteristics and histologic properties of the synthesized materials were investigated by thermal (TG-DSC) analysis, powder X-ray diffraction (XRD) analysis, Fourier transform infrared (FTIR) spectroscopy, scanning electron microscopy (SEM), and microcomputer tomography (microCT).

## II. EXPERIMENTAL

$\beta$ -TCP powders were synthesized using wet polymeric precipitation chemical method in an aqueous PVA (partially hydrolyzed, Mw approx. 70000) solution. In the synthesis, calcium nitrate tetrahydrate and diammonium hydrogen phosphate were used as a source of Ca and P, respectively. The Ca/P ratio was fixed 1.5. Reaction pH was controlled using ammonia solution (25%). Firstly, calcium nitrate tetrahydrate (0.013425 mol) was dissolved in 1% aqueous PVA solution, and 10 mL of ammonia solution was added.

Secondly, diammonium hydrogen phosphate (0.00895 mol) was dissolved in 30 mL of deionized water and quickly poured to the above solution of calcium nitrate. After mixing for 10 min (750 rpm), the precipitate was filtered and washed with deionized water (3x 30 mL) having 2 ml ammonia solution and later only with deionized water (3x10 mL). After drying of precipitates at 120 °C for 3h, the obtained amorphous powders were heated at 800 for 5h with a heating rate of 1 °C/min.

The thermal decomposition of the precipitated species was analyzed through thermogravimetric analysis and differential scanning calorimetry (TG-DSC) using Perkin Elmer STA 6000 Simultaneous Thermal Analyzer. Dried samples of about 5–10 mg were heated from 25 to 950 °C at a heating rate of 10 °C/min in a dry flowing air (20 mL/min). X-ray powder diffraction (XRD) measurements were carried out on Rigaku MiniFlex II diffractometer working in Bragg-Brentano ( $\theta/2\theta$ ) geometry using Ni-monochromatized  $\text{CuK}\alpha$  radiation. Lattice parameters are refined by the Rietveld method using the FullProf program. Lattice-parameter refinement was carried out assuming the rhombohedral space group, R3c (no. 161), expected for  $\beta$ -TCP structure [23], [24]. The crystallite size of the synthesized  $\beta$ -TCP was calculated from the broadening in the XRD pattern by the Scherrer's formula,  $d = 0.89 \lambda / B \cos\theta$ , where  $\lambda$  is the X-ray wavelength,  $\theta$  is the maximum intensity of an observed peak, and  $B$  is defined as the full width of the peak from the intensity distribution pattern measured at half of the maximum intensity (FWHM) value [25]. Infrared spectra were recorded using Fourier transform infrared (FT-IR) spectrometer (Frontier FT-IR, PerkinElmer) equipped with Gladi attenuated total reflection (ATR) viewing plate (Diamond ATR crystal), MCT detector (4000-500  $\text{cm}^{-1}$ , 25 scans). The morphology of the final powders and films was characterized by scanning electron microscopy performed with a Hitachi SU-70 field-emission scanning electron microscope (FE-SEM). For the histological investigation the  $\beta$ -TCP specimens (0.23 g) were mixed with ethanol and pressed by mechanical press using a pressure of 1 ton for 10 minutes to the bars. A cross-sectional image of the obtained specimens was taken by a micro-CT scanner (Skyscan 1076, Belgium). High-resolution scanning, with an in-plane pixel size and thickness of 9  $\mu\text{m}$ , was performed. The micro-CT scanners built-in software was used to make a 3-D reconstruction from the set of scans.

### III. RESULTS AND DISCUSSION

The thermal decomposition behaviour of precipitated Ca-P-O PVA precursor, corresponding to the final composition of  $\text{Ca}_3(\text{PO}_4)_2$ , was investigated by simultaneous TG-DSC measurements. The TG-DSC curves of precipitated Ca-P-O PVA precursor are shown in Fig. 1.

As seen, the thermal decomposition of obtained precipitate passes through four stages. The first weight loss (0.5%) in the TG curve from room temperature to 100 °C is due to the loss of residual water in the precipitate [26]. This weight loss is accompanied by broad endothermic peak in DSC curve. The

second weight loss (6%) observed in the TG curve in the range of about 100–400 °C can be ascribed to the decomposition of polymeric matrix. The third monotonical weight change (~1.5%) in the temperature range of 400–740 °C is attributed to the final decomposition of residual of organic part [26]. The weak endothermic signals in DSC curve confirm the decomposition processes which take place in this temperature interval. The final weight loss of 0.8% peaked at about 750 °C probably indicates a decomposition of intermediate  $\text{CaCO}_3$ . No more weight changes are observed above 750 °C, indicating that all organic residues and carbonates are decomposed at this point. The exothermic peaks above 750 °C in DSC curve are attributed to amorphous-crystalline phase transition in CaO and formation of  $\text{Ca}_3(\text{PO}_4)_2$ . Thus, thermal analysis results suggested that the final annealing temperature 800 °C should be selected for the synthesis of  $\beta$ -TCP.

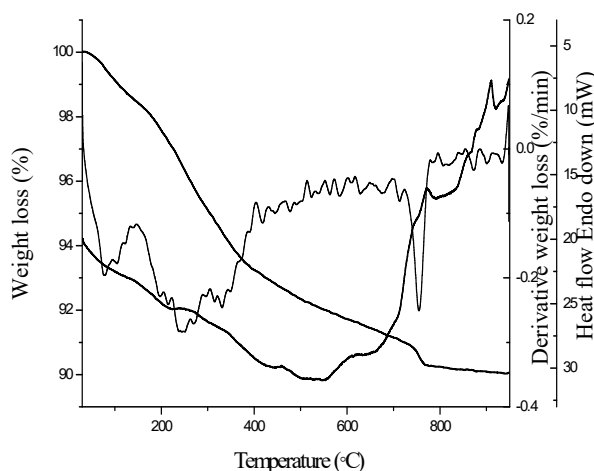


Fig. 1 TG-DSC and DTG curves of precipitated Ca-P-O PVA precursor

The FTIR spectra of the dried Ca-P-O PVA precursor and final product are presented in Fig. 2.

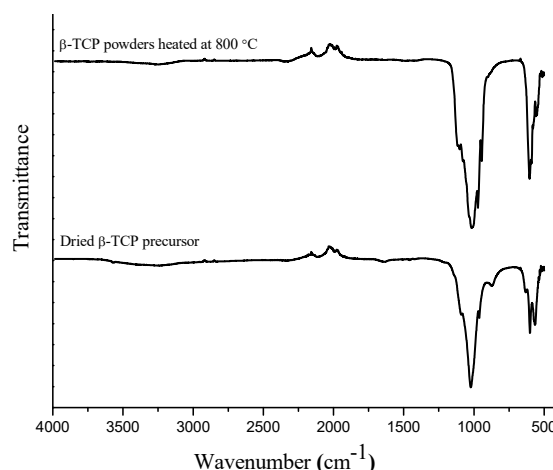


Fig. 2 FTIR spectra of the dried Ca-P-O PVA precursor and final product obtained after annealing at 800 °C

In both FTIR spectra, the absorption peaks in the range of  $1100\text{--}950\text{ cm}^{-1}$  attributable to the P-O vibrations in  $\text{PO}_4^{3-}$  ( $\text{Ca}_3(\text{PO}_4)_2$ ) [27], [28] are clearly visible. In the IR spectrum of Ca-P-O PVA precursor, a broad absorption band located at  $3600\text{--}3200\text{ cm}^{-1}$  could be attributed to O-H stretch vibration in alcohol (PVA). However, C-O stretching vibrations ( $1150\text{--}1050\text{ cm}^{-1}$ ) perhaps overlap with the P-O vibration. Intensive absorption lines located at  $600\text{ cm}^{-1}$  unambiguously could be attributed to Ca-O vibrations in phosphate structure. Bands at ca.  $2350\text{ cm}^{-1}$  belong to carbon dioxide from atmosphere [29]. Therefore, the FTIR spectra indicate the presence of phosphates in the samples. Additionally, the peak attributable to the P-O vibrations is more intensive for the sample obtained after heating at  $800^\circ\text{C}$ .

The phase crystallinity and purity of the samples were characterized by means of XRD analysis. Fig. 3 shows the XRD patterns of the dried as-synthesized  $\beta$ -TCP precursor and powders subsequently annealed at elevated temperatures.

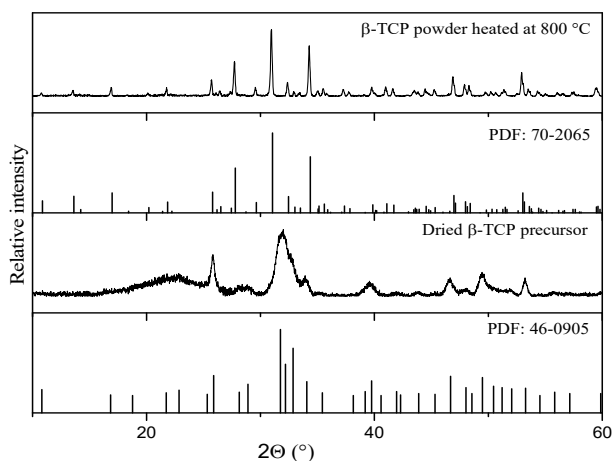
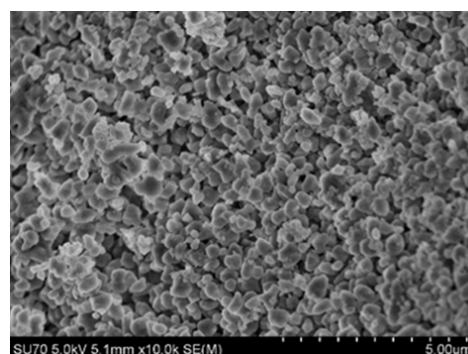


Fig. 3 XRD patterns of the dried Ca-P-O PVA precursor and final product obtained after annealing at  $800^\circ\text{C}$ . Vertical lines represent standard XRD patterns of  $\beta$ -TCP (at top) and CHA (at bottom)

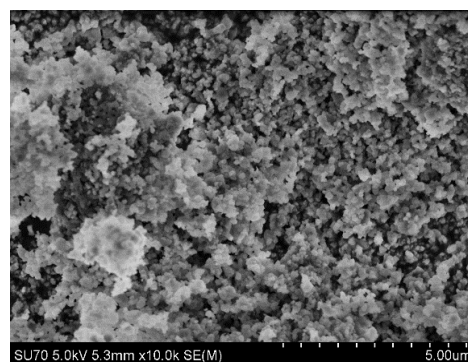
It can be seen that the obtained precursor was already a poor crystalline compound; however, the diffraction peaks appear relatively low and broad. The diffraction peaks are considered to arise from the apatite-like crystals according to JCPDS file no. 00-46-0905 [21]–[23]. With continuously increasing the calcination temperature to  $800^\circ\text{C}$  (Fig. 3), the target  $\beta$ -TCP phase (JCPDS file no. 00-09-0169) was obtained as the main phase as shown in the bottom of Fig. 3 by vertical lines [21], [22]. All the characteristic peaks matched well with the corresponding hkl standard planes. Major  $\beta$ -TCP peaks are labelled in Fig. 3. Thus, the nanocrystalline CDHA phase has transformed into  $\beta$ -TCP, similar to the results published previously [21], [22]. Based on the obtained XRD results, we can conclude that the phase formation mechanism in co-precipitated specimens is similar to the traditional synthesis route presented by (1). The crystallite sizes were calculated to be less than  $100\text{ nm}$  for both as-prepared and heat-treated samples.

The morphology of as-synthesized  $\beta$ -TCP precursor and

synthesized  $\beta$ -TCP powders were examined using scanning electron microscopy (SEM). The SEM micrographs of  $\beta$ -TCP samples synthesized by polymeric precipitation method are shown in Fig. 4.

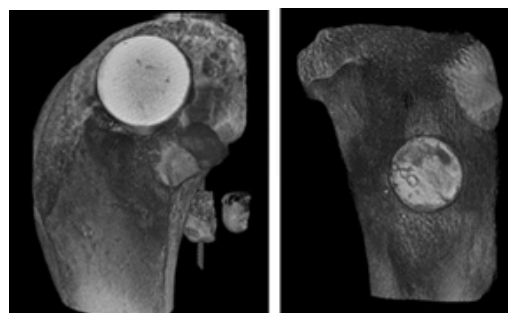


(a)



(b)

Fig. 4 SEM micrographs obtained of the dried Ca-P-O PVA precursor (a) and synthesized  $\beta$ -TCP (b)



(a)

(b)

Fig. 5 MicroCT images of  $\beta$ -TCP specimen placed in the bones: femur (a) and tibia (b)

The SEM images clearly demonstrate that the as-synthesized  $\beta$ -TCP powders consist of irregularly-shaped small particles covered by amorphous accumulation of clouds [30]. The spherical shape particles  $100\text{--}300\text{ nm}$  in size of  $\beta$ -TCP have formed after heat treatment at  $800^\circ\text{C}$ . It is evident that the synthesized  $\beta$ -TCP powders show narrow and

homogeneous particle size distribution although it had been ground manually in a mortar [31]. From these  $\beta$ -TCP powders, the bars of 6.46 x 4.35 mm size were pressed for further animal in situ investigations. Fabricated  $\beta$ -TCP specimens were placed to the holes drilled in the bones of the rats and will be maintained from four weeks to two months. The microcomputer tomography images of  $\beta$ -TCP samples inserted in to the bones are shown in Fig. 5.

The histological characterization of removed  $\beta$ -TCP samples are under investigation.

#### IV. CONCLUSION

In the present work, for the synthesis of tricalcium phosphate ( $\beta$ -Ca<sub>3</sub>(PO<sub>4</sub>)<sub>2</sub>,  $\beta$ -TCP) powders a novel wet polymeric precipitation method has been developed. The formation of  $\beta$ -TCP ceramics synthesized by polymeric precipitation method requires 800 °C temperature, as determined by TG/DSC analysis. The XRD analysis results confirmed that single phase  $\beta$ -TCP powders were obtained at rather low temperature (800 °C). Moreover, formation of  $\beta$ -TCP occurred via transformation of the nanocrystalline CDHA phase into  $\beta$ -TCP. The SEM micrographs of  $\beta$ -TCP samples synthesized by polymeric precipitation method showed that spherically shaped particles 100–300 nm in size have formed after heat treatment at 800 °C. Besides, the synthesized  $\beta$ -TCP powders showed narrow and homogeneous particle size distribution. The histological characterization of  $\beta$ -TCP samples will be performed.

#### REFERENCES

- [1] M. Winter, P. Griss, K. de Groot, H. Tagai, G. Heimke, HJ von Dijk, K. Sawai. "Comparative histocompatibility testing of seven calcium phosphate ceramics", *Biomater.*, vol. 2, pp. 159–160, 1981.
- [2] N. Passuti, G. Daculsi, J.M. Rogez, S. Martin, J.V. "Bainvel. Macroporous calcium phosphate ceramic performance in human spine fusion". *Clin. Orthop. Relat. Res.*, vol. 248, pp. 169–176, 1989.
- [3] S.-I. Roohani-Esfahani, Y.J. No, Z.F. Lu, P.Y. Ng, Y.J. Chen, J. Shi, N.J. Pavlos, H. Zreiqat. "A bioceramic with enhanced osteogenic properties to regulate the function of osteoblastic and osteoclastic cells for bone tissue regeneration", *Biomed. Mater.*, vol. 11, 2016, p.035018.
- [4] M. Bohner, "Calcium orthophosphates in medicine: from ceramics to calcium phosphate cements". *Injury*, vol. 31, pp. SD37–SD47, 2000.
- [5] S.V. Dorozhkin, M. Epple. "Biological and medical significance of calcium phosphates", *Angew. Chem. Int. Ed. Engl.*, vol. 41, pp. 3130–3146, 2002.
- [6] T. Takahata, T. Okihara, Y. Yoshida, K. Yoshihara, Y. Shiozaki, A. Yoshida, K. Yamane, N. Watanabe, M. Yoshimura, M. Nakamura, M. Irie, B. Van Meerbeek, M. Tanaka, T. Ozaki, A. Matsukawa. "Bone engineering by phosphorylated-pullulan and beta-TCP composite". *Biomed. Mater.*, vol. 10, p. 065009, 2015.
- [7] G. Tozzi, A. De Mori, A. Oliveira, M. Roldo. "Composite hydrogels for bone regeneration" *Mater.*, vol. 9, UNSP 267, 2016.
- [8] J. Kolmas, S. Krukowski, A. Laskus, M. Jurkiewicz. "Synthetic hydroxyapatite in pharmaceutical applications," *Ceram. Int.*, vol. 42, pp. 2472–2487, 2016.
- [9] S. Utech, A.R. Boccaccini. "A review of hydrogel-based composites for biomedical applications: enhancement of hydrogel properties by addition of rigid inorganic fillers," *J. Mater. Sci.*, vol. 51, pp. 271–310, 2016.
- [10] R.Z. Le Geros, "Properties of osteoconductive biomaterials: calcium phosphates". *Clin. Orthop.*, vol. 395 pp. 81–98, 2002.
- [11] D.S. Metzger, T.D. Driskell, J.R. Paulsrud. "Tricalcium phosphate ceramic—a resorbable bone implant: review and current status", *J. Am. Dent. Assoc.*, vol. 105, pp. 1035–1038, 1982.
- [12] J.X. Lu, A. Gallur, B. Flautre, K. Anselme, M. Descamps, B. Thierry, P. Hardouin. "Comparative study of tissue reactions to calcium phosphate ceramics among cancellous, cortical, and medullar bone sites in rabbits", *J. Biomed. Mater. Res.*, vol. 42, pp. 357–367, 1998.
- [13] M. Bohner, G.H. Lenthe, S. Gruenfelder, W. Hirsiger, R. Evison, R. Mueller. "Synthesis and characterization of porous beta-tricalcium phosphate blocks", *Biomater.*, vol. 26, pp. 6099–6105, 2005.
- [14] DSH Lee, Y. Pai, S. Chang, D.H. Kim. "Microstructure, physical properties, and bone regeneration effect of the nano-sized  $\beta$ -tricalcium phosphate granules", *Mater. Sci. Eng. C.*, vol. 58, pp. 971–976, 2016.
- [15] K. Ishikawa, N. Koga, K. Tsuru, I. Takahashi. "Fabrication of interconnected porous calcite by bridging calcite granules with dicalcium phosphate dihydrate and their histological evaluation", *J. Biomed. Mater. Res. Part A.*, vol. 104, pp. 652–658, 2016.
- [16] Y. Pan, J.L. Huang, C.Y. Shao. "Preparation of  $\beta$ -TCP with high thermal stability by solid reaction route", *J. Mater. Sci.*, vol. 38, pp. 1049–1056, 2003.
- [17] J.S. Cho, D.S. Jung, J.M. Han, Y.C. Kang. "Nano-sized  $\alpha$  and  $\beta$ -TCP powders prepared by high temperature flame spray pyrolysis", *Mater. Sci. Eng. C.*, vol. 29, pp. 1288–1292, 2009.
- [18] K.P. Sanosh, M.C. Chu, A. Balakrishnan, T.N. Kim, S.J. Cho, "Sol-gel synthesis of pure nano sized b-tricalcium phosphate crystalline powders", *Curr. Appl. Phys.*, vol. 10, pp. 68–71, 2010.
- [19] S.C. Liou, S.Y. Chen. "Transformation mechanism of different chemically precipitated apatitic precursors into  $\beta$ -tricalcium phosphate upon calcinations", *Biomater.*, vol. 23, pp. 4541–4547, 2002.
- [20] D.R.R. Lazar, S.M. Cunha, V. Ussui, E. Fancio, N.B. de Lima, A.H.A. Bressiani. "Effect of calcination conditions on phase formation of calcium phosphates ceramics synthesized by homogeneous precipitation", *Mater. Sci. Forum.*, vol. 530, pp.612–617, 2006.
- [21] M. Akao, H. Aoki, K. Kato, A. Sato. "Dense polycrystalline b-tricalcium phosphate for prosthetic applications", *J. Mater. Sci.*, vol. 17 343–346, 1982.
- [22] A. Destainville, E. Champion, D. Bernache-Assollant, E. Laborde. "Synthesis, characterization and thermal behavior of apatitic tricalcium phosphate", *Mater. Chem. Phys.*, vol. 80, pp. 269–277, 2003.
- [23] S.C. Liou, S.Y. Chen, H.Y. Lee, J.S. Bow. "Structural characterization of nano-sized calcium deficient apatite powders", *Biomater.*, vol. 25, pp. 189–196, 2004.
- [24] B. Dickens, L.W. Schroeder, W.E. Brown. "Crystallographic studies of the role of Mg as a stabilizing impurity in  $\beta$ -Ca<sub>3</sub>(PO<sub>4</sub>)<sub>2</sub>. The crystal structure of pure  $\beta$ -Ca<sub>3</sub>(PO<sub>4</sub>)<sub>2</sub>", *J. Solid State Chem.*, vol. 10, pp. 232–248, 1974.
- [25] R. Jenkins, R.L. Snyder. *Chemical Analysis: Introduction to X-ray Powder Diffractometry*, Wiley, New York (1996) p. 90.
- [26] I. Bogdanoviciene, M. Cepenko, R. Traksmas, A. Kareiva, K. Tõnsuaadu. "Formation of Ca-Zn-Na phosphate bioceramic material in thermal processing of EDTA sol-gel precursor", *J. Therm. Anal. Calorim.*, vol. 121, pp. 107–114, 2015.
- [27] E. Garskaite, L. Alinauskas, M. Drienovsky, J. Krajcovic, R. Cicka, M. Palcut, L. Jonusauskas, M. Malinauskas, Z. Stankeviciute, A. Kareiva. "Fabrication of composite of nanocrystalline carbonated hydroxyapatite (cHAP) with polylactic acid (PLA) and its surface topographical structuring with direct laser writing (DLW)", *RSC Adv.*, vol.6, ppt. 72733–72743, 2016.
- [28] J. Trinkunaite-Felsen, Z. Stankeviciute, J.C. Yang, T.C.K. Yang, A. Beganskiene, A. Kareiva. "Calcium hydroxyapatite/whitlockite obtained from dairy products: simple, environmentally benign and green preparation technology", *Ceram. Int.*, vol. 40, pp. 12717–12722, 2014.
- [29] A. Gatelyte, D. Jasaitis, A. Beganskiene, A. Kareiva. "Sol-gel synthesis and characterization of selected transition metal nano-ferrites. *Materials Science (Medžiagotyra)*", vol. 17, pp. 302–307, 2011.
- [30] S. Hosseini, H. Naderi-Manesh, H. Vali, S. Faghihi. "Improved surface bioactivity of stainless steel substrates using osseocalcin mimetic peptide", *Mater. Chem. Phys.*, vol. 143, pp. 1364–1371, 2014.
- [31] M.Koizhaiganova, I. Yasa, G. Gulumser. "Characterization and antimicrobial activity of silver doped hydroxyapatite obtained by the microwave method. *Materials Science (Medžiagotyra)*", vol. 22, pp. 403–408, 2016.